

# Degradation of Organic Dyes over Polymeric Photocatalyst $C_3N_3S_3$

Yin Junyao

School of Materials Science and Technology  
Harbin University of Science and Technology, HUST  
Harbin, P. R. China  
e-mail: 708899815@qq.com

Xu Huanyan\*

School of Materials Science and Technology  
Harbin University of Science and Technology, HUST  
Harbin, P. R. China  
\*Corresponding Author. e-mail: xhy7587@aliyun.com

**Abstract—Objective:** Due to the good visible-light response and strong electron transfer ability, the polymeric semiconductor  $C_3N_3S_3$  was developed as an inspired photocatalyst for the degradation of organic dyes. **Methods:** Trithiocyanuric acid was used as the raw material for the synthesis of  $C_3N_3S_3$  by hydrolytic method in NaOH-KI mixed solution. X-ray diffraction, Fourier transform infrared spectroscopy, scanning electron microscopy and ultraviolet-visible diffuse reflectance spectroscopy were employed to identify the obtained product. Organic dyes with different characteristics were used to evaluate the photocatalytic activity of  $C_3N_3S_3$ . **Results:** The characterization results revealed that the obtained sample had the stable structure of  $C_3N_3S_3$  polymer with the band gap of 2.67eV, which is one of the characteristics of conductors. The photocatalytic tests showed that  $C_3N_3S_3$  polymer had good photocatalytic activity and adsorption capacity, especially for the cationic dyes. Furthermore, the photocatalytic activity was better when the pH value of dyeing solution was 5. **Conclusion:** Polymeric semiconductor  $C_3N_3S_3$  showed good photocatalytic activity for the degradation of organic dyes, which would be one of the most important materials for the environmental remediation and pollution control.

**Keywords-** $C_3N_3S_3$ ; Polymeric photocatalyst; Organic dyes; Photocatalytic activity; Adsorption capacity

## I. INTRODUCTION

With the rapid development of the world economy, energy and environmental issues have become major factor which restrict the development economic and social of all countries [1], which is a serious problem of sustainable development which human must face. In modern industrial production, due to a variety of drugs and chemical products was abused and second products was burnt that lead to a lot of pollutants seriously stack in the environment, and pollutants usually is very stable chemical properties that can exist for a long time in the environment, which have been seriously threaten human health [2]. Because of pollutants possess features that are complex chemical composition and poor biodegradable which lead it difficult to degrade with traditional methods. Developing and utilizing new energy, while controlling and governing environmental pollution has become a major issue which human society need to be resolved. As it possessed excellent optical properties, catalytic properties, and photoelectric conversion performance [3], semiconductor

photocatalytic material has caused general interest of the scientific community. Due to be able to use solar energy to achieve energy conversion and pollutant degradation [4, 5], developing semiconductor photocatalytic materials and photocatalytic technology is expected to be an effective way to solve environmental and energy problems [6-9]. So, semiconductor photocatalytic materials and photocatalytic technology to solve energy, pollution has important practical significance [10, 11].

Now, represent by  $TiO_2$ , the semiconductor photocatalytic oxidation technology has very broad application prospects in the manufacture of new energy and protective of environmental in the field of air and water purification [12]. However, the photocatalyst is low of quantum efficiency and narrow of optical response range, which issue has been restricted large-scale application of this technology [13]. The current focus issue of photocatalytic science is exploring new and efficient photocatalytic materials, improving the photocatalytic efficiency and revealing the nature of the photocatalytic process, then the organic polymer photocatalytic materials is the hot research direction. Inspired polymer  $C_3N_4$  photocatalytic materials [14, 15] discovered by the latest international. Buildd polymeric triazine ring by double or single sulfur bond with a large  $\pi$  bond structure[16]. Thinked by absorb visible light and strong electron transfer ability of organic polymer to preparation polymer  $C_3N_3S_3$ . Photocatalytic materials is an innovative exploration, photocatalytic materials  $C_3N_3S_3$  polymer is prepared which it is still deep space of research, the findings of the study has important scientific significance for rich of the photocatalytic scientific foundation and development of new polymer-based photocatalytic materials [17].

Metal-free carbon-based hybrids composed of reduced graphene oxide (rGO) and  $C_3N_3S_3$  polymers with a layered "sandwich" structure were fabricated by an in situ two-step polymerization strategy and used as visible light photocatalysts for selective aerobic oxygenation of benzylic alcohols to the corresponding aldehydes, at good efficiency and high selectivity [18]. In this work, trithiocyanuric acid was used as the raw material for the synthesis of  $C_3N_3S_3$  by hydrolytic method in NaOH-KI mixed solution. X-ray diffraction, Fourier transform infrared spectroscopy, scanning electron microscopy and ultraviolet-visible diffuse reflectance spectroscopy were

employed to identify the obtained product. Organic dyes with different characteristics were used to evaluate the photocatalytic activity of  $C_3N_3S_3$ .

## II. EXPERIMENTAL SECTION

### A. $C_3N_3S_3$ Synthesis

The synthesis of  $C_3N_3S_3$  was conducted by a simple route. Generally, trithiocyanuric acid was dissolved in 100 ml of water containing 0.06 mol of NaOH. Then 0.03 mol of iodine in a concentrated aqueous solution of KI was slowly added at 0 °C and the mixture was stirred overnight. A yellowish precipitate was washed with deionized water several times to remove residual ions, and finally dried under vacuum at 60 °C.

### B. $C_3N_3S_3$ Characterization

X-ray diffraction (XRD), Fourier transform infrared spectroscopy (FT-IR) and scanning electron microscopy (SEM) were employed to identify the composition, morphology and structure of the obtained  $C_3N_3S_3$  polymer. The band gap of sample was determined by ultraviolet-visible diffuse reflectance spectroscopy (DRS).

### C. Photocatalytic tests

A 300W Xe lamp was used as the light source. In a typical reaction, 100 mL solution with certain dosage of catalyst was injected into a 200 mL glass bottle. The mixture was magnetically stirred for 2.5 h under dark to obtain adsorption/desorption equilibrium of organic dye on the catalyst. The solution was then exposed to the Xe lamp. At time intervals of 0.5 h, 2 mL sample was collected from the mixture and filtered, then the filtered solution was measured the concentration of organic dye, using a 721-type UV-vis spectrophotometer. The discoloration ratio, i.e. the removal degree of color at the maximum absorption wavelength of organic dyes was calculated using  $D_R (\%) = (C_0 - C_t) / C_0 \times 100$ , where  $C_0$  is the initial concentration of the organic dye and  $C_t$  the concentration at irradiation time  $t$ . In order to check the reproducibility of the results, random tests were done for different experimental conditions.

## III. RESULTS AND DISCUSSION

### A. Characterization results

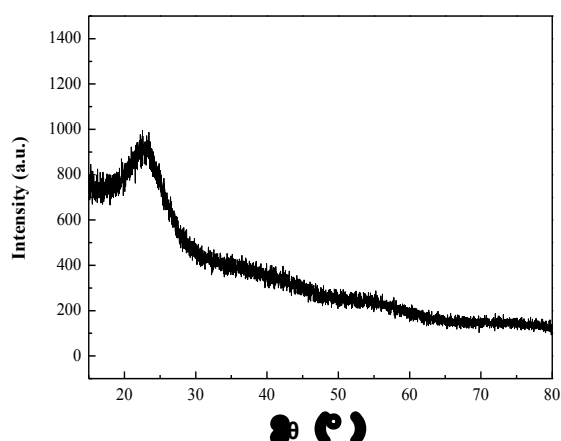


Figure 1. XRD pattern of  $C_3N_3S_3$

The XRD pattern of  $C_3N_3S_3$  polymer is shown in Figure 1, where it can be seen that only one broadened diffraction peak exist at 22.9°, indicating that the resulting solid is an amorphous material. The position of XRD pattern peak is same to that reported by Long's group [19], implying that the obtained substance was  $C_3N_3S_3$ .

As shown in Figure 2, the FTIR spectrum of trithiocyanuric acid is well consistent with that reported in literature. The major bands observed at 1540, 1125, and 750  $cm^{-1}$  in the IR spectrum belong to the characteristic of the nonaromatic, thirthione consisting of the triazine ring. Specifically, 1125  $cm^{-1}$  is assigned to C=S stretching vibrations. The peaks at the position of 2900~3160  $cm^{-1}$  are attributed to -N-H stretching vibrations. After oxidative polymerization of trithiocyanuric acid, both of peaks at 2900~3160 and 1125  $cm^{-1}$  disappear in the IR spectrum. On the other hand, the characteristic peaks around 1479, 1248, and 827  $cm^{-1}$  of the aromatic, trithiol form of the ring appear, as found in the spectrum of trithiocyanurate. This indicates that polymer  $C_3N_3S_3$  is successfully synthesized.

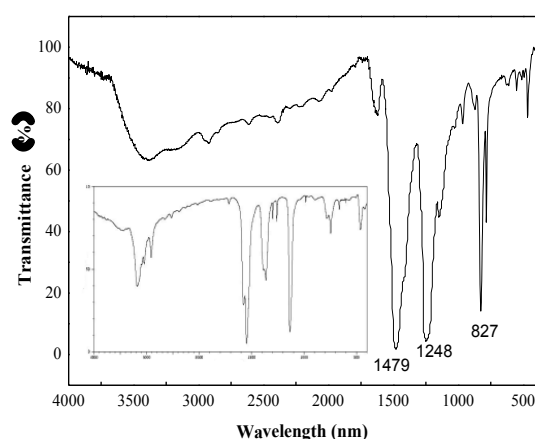


Figure 2. FTIR spectra of  $C_3N_3S_3$  and trithiocyanuric acid (inset)

SEM observation of as-prepared product is shown in Figure 3, where it can be seen that the shape of product particles is irregular with different diameters. The particles exhibit irregular shapes and they desultorily aggregate together.

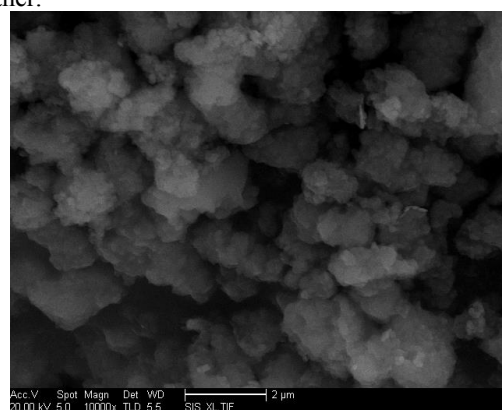


Figure 3. SEM image of  $C_3N_3S_3$

The ultraviolet-visible diffuse reflectance spectrum (Figure 4) clearly indicates an absorption band edge with the semiconducting feature at 400 nm. As can be seen

from the inset, the band gap is 2.627eV, which are consistent with the relevant literature analysis.

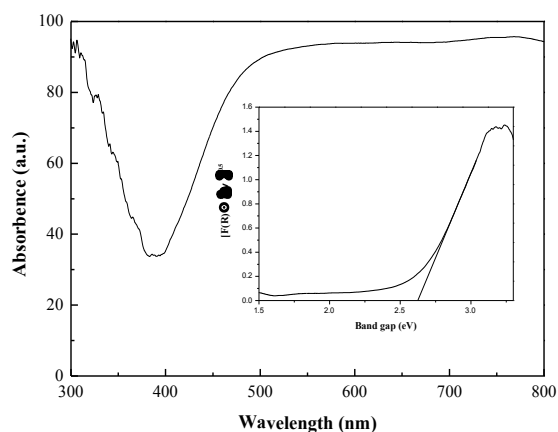


Figure 4. DRS Pattern of  $C_3N_3S_3$  and its calculation of band gap (inset)

### B. Photocatalytic Evaluation

As can be seen from the Figure 5, the prepared sample has particularly strong absorption for the two cationic dye, Rhodamine B (RhB) and Methylene Blue (MB), proving that the surface of the sample is negatively charged. The discoloration ratio attributed to adsorption is over 90%. The adsorption effect of sample prepared is particularly poor to magenta, the experimental results is not easy to be seen. The adsorption effect of prepared sample is moderate to methyl orange, that the experimental results is easy to be seen, so Methyl Orange (MO) was chosen to evaluate the photocatalytic activity of  $C_3N_3S_3$ .

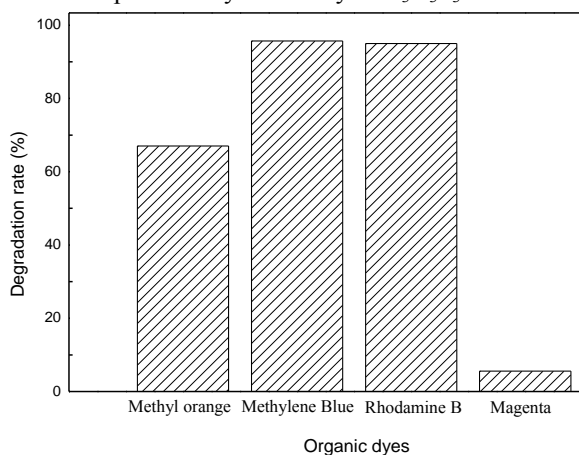


Figure 5. Adsorption of different organic dyes onto  $C_3N_3S_3$

As shown in Figure 6, the effect of solution pH on the photocatalytic activity of  $C_3N_3S_3$  was conducted in this study. Other reaction conditions remain unchanged, 0.1g of  $C_3N_3S_3$  were added to the 100mL solution of methyl orange (5mg / L) which were different of PH at 3, 5, 7, 9, and 11. After 2.5h reached equilibrium, the decolorization rate of methyl orange were 88.7%, 56.5%, 48.3%, 17.0%, and 15.7%. After irradiated by ultraviolet (UV) light for 1.5 h, the decolorization rate of methyl orange were 92.1%, 80.8%, 52.8%, 36.7% and 20.2%. It can be seen that the decolorization rate was under acidic conditions significantly better than under alkaline conditions. The

reason for this phenomenon might be that the surface charge properties of  $C_3N_3S_3$  changed with pH.

The Figure 7 shows that the effect of different amounts of sample  $C_3N_3S_3$  on photocatalytic degradation of methyl orange. The amount of  $C_3N_3S_3$  was 0.1g, 0.2g, 0.3g, and 0.4g, respectively, which added to the 100mL solution methyl orange (5mg / L), After 2.5h reached equilibrium, the decolorization rate of methyl orange were 5.8%, 26.4%, 38.0%, and 49.8%. After irradiated by ultraviolet (UV) light for 1.5 h, the decolorization rate of methyl orange were 13.8%, 2.1% , 49.8% and 58.5%. It can be seen, as the amount of catalyst is increased, the decolorization of methyl orange becomes is better. MO discoloration ratio increased with catalyst dosage increasing. The possible reason for this phenomenon might be attributed to the fact that, with catalyst dosage increasing, the active sites on the photocatalyst surface increased and accordingly reactive species increased [20].

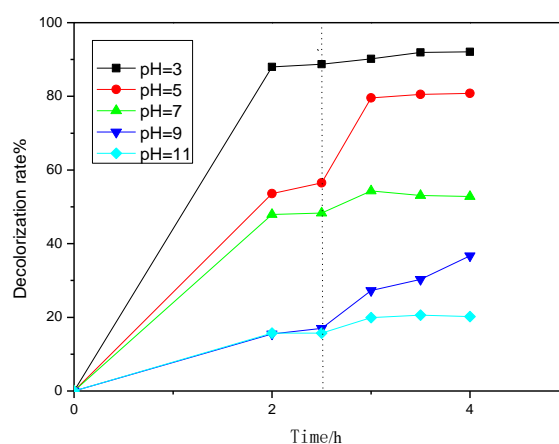


Figure 6. Impact of solution pH on MO photocatalytic discoloration

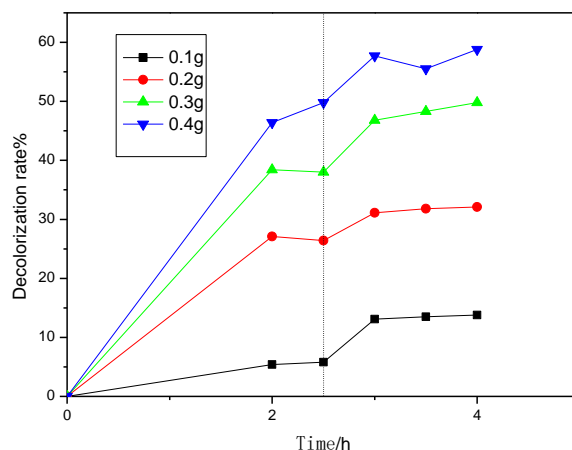


Figure 7. Impact of catalyst dosage on MO photocatalytic discoloration

Figure 8 shows the effect of MO initial concentration on the photocatalytic degradation of MO. Added 0.1g of  $C_3N_3S_3$  in 100mL of the different concentration solution of methyl orange were 5mg / L, 10 mg / L, 20 mg / L, and 30 mg/L. After 2.5h reached equilibrium, the decolorization rate of methyl orange were 9.1%, 7.8%, 7.6% and 3.1%. After irradiated by ultraviolet (UV) light for 1.5 h, the decolorization rate of methyl orange were 8.2%, 12.7%, 10.6% and 7.4%. As the concentration of catalyst is increased, the decolorization of methyl orange becomes is

worse. The slight decrease of photocatalytic discoloration efficiency with an increase in MO initial concentration might be attributed to several factors. Firstly, higher dye concentration made more adsorbed dye molecules occupy the active sites of TiO<sub>2</sub> surface. This suggested that as the dye concentration increased, more and more dye molecules would be adsorbed on the surface of the photocatalyst. Accordingly, generation of the reactive species ( $\bullet\text{OH}$  and  $\bullet\text{O}_2$ ) needed for the degradation of the dye decreased; secondly, more intermediates would be generated at higher dye concentration, which could also be adsorbed on the surface of the solid catalyst. Slow diffusion of the generated intermediates from the catalyst surface could lead to the deactivation of the photocatalyst and consequently, a reduction in the degradation efficiency; thirdly, at higher dye concentration, more absorption of light photon by the dye itself resulted in a lesser availability of photons for reactive species generation [21].

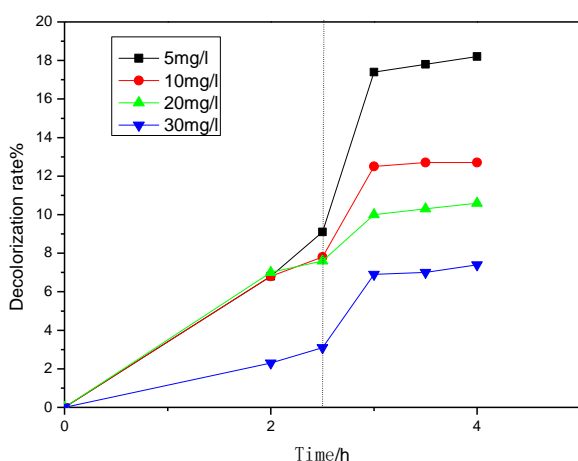


Figure 8. Impact of MO initial concentration on its photocatalytic discoloration

#### IV. CONCLUSION

In summary, the characterization results revealed that the obtained sample had the stable structure of C<sub>3</sub>N<sub>3</sub>S<sub>3</sub> polymer with the band gap of 2.67eV, which is one of the characteristics of conductors. The photocatalytic tests showed that C<sub>3</sub>N<sub>3</sub>S<sub>3</sub> polymer had good photocatalytic activity and adsorption capacity, especially for the cationic dyes. Furthermore, the photocatalytic activity was better when the pH value of dyeing solution was 5.

#### ACKNOWLEDGMENT

This work was financially supported by the Program for New Century Excellent Talents in Heilongjiang Provincial Universities (1253-NCET-010).

#### REFERENCES

- [1] A. Kudo, and Y. Miseki. Heterogeneous photocatalyst materials for water splitting. *Chemical Society Reviews*, 2009, 38(1): 253-278.
- [2] B. Liu, X. L. Liu, and N. S. Deng. The photocatalytic degradation of 17 alpha-ethynylestradiol(EE2) with Anaabaena. *Acta Hydrobiologica Sinica*, 2003, 27(4): 390-395.
- [3] J. Yu, J. Fan, and K. Lv. Anatase TiO<sub>2</sub> nanosheets with exposed (001) facets: improved photoelectric conversion efficiency in dye-sensitized solar cells. *Nanoscale*, 10 (2010): 2144-2149.
- [4] X. B. Chen, and S. S. Mao. Titanium dioxide nanomaterials: Synthesis, properties, modifications and applications *Chemical Reviews*, 2007, 107 (7): 2891-2959.
- [5] X. Dang, X. Zhang, Z. Lu, et al. Construction of Au@TiO<sub>2</sub>/graphene nanocomposites with plasmonic effect and super adsorption ability for enhanced visible-light-driven photocatalytic organic pollutant degradation. *Journal of nanoparticle research*, 2014, 16: 2215-2220.
- [6] Y. Liang, S. Lin, L. Liu, et al. Oil-in-water self-assembled Ag@AgCl QDs sensitized Bi<sub>2</sub>WO<sub>6</sub>: Enhanced photocatalytic degradation under visible light irradiation. *Applied Catalysis B: Environmental*, 2015, 164: 192-203.
- [7] A. Ren, C. Liu, Y. Hong, et al. Enhanced visible-light-driven photocatalytic activity for antibiotic degradation using magnetic NiFe<sub>2</sub>O<sub>4</sub>/Bi<sub>2</sub>O<sub>3</sub> heterostructures. *Chemical Engineering Journal*, 2014, 258: 301-308.
- [8] S. W. Hu, L. W. Yang, Y. Tian, et al. Non-covalent doping of graphitic carbon nitride with ultrathin graphene oxide and molybdenum disulfide nanosheets: An effective binary heterojunction photocatalyst under visible light irradiation. *Journal of Colloid and Interface Science*, 2014, 431: 42-49.
- [9] Y. Luo, X. Liu, X. Tang, et al. Gold nanoparticles embedded in Ta<sub>2</sub>O<sub>5</sub>/Ta<sub>3</sub>N<sub>5</sub> as active visible-light plasmonic photocatalysts for solar hydrogen evolution. *Journal of Materials Chemistry A*, 2014, 2: 14927-14939.
- [10] L. Ye, Y. Su, X. Jin, et al. Recent advances in BiOX (X=Cl, Br and I) photocatalysts: synthesis, modification, facet effects and mechanisms. *Environmental Science: Nano*, 2014, 1: 90-112.
- [11] G. Zhu, M. Hojamberdiev, C. Tan, et al. Photodegradation of organic dyes with anatase TiO<sub>2</sub> nanoparticles-loaded BiOCl nanosheets with exposed {001} facets under simulated solar light. *Materials Chemistry and Physics*, 2014, 147: 1146-1156.
- [12] C. L. Miao, and H. Wang. Study on Degradation of Dyes Wastewater by N-Doped TiO<sub>2</sub>. *Advanced Materials Research*, 2013, 634: 263-266.
- [13] T. B. Nguyen, M. J. Hwang, and K. S. Ryu. Synthesis and High Photocatalytic Activity of Zn-doped TiO<sub>2</sub> Nanoparticles by Sol-gel and Ammonia-Evaporation Method. *Bulletin of Korean Chemical Society*, 2012, 33: 243-247.
- [14] Y. Wang, H. R. Li, J. Yao, et al. Synthesis of boron doped polymeric carbon nitride solids and their use as metal-free catalysts for aliphatic C-H bond oxidation. *Chemical Science*, 2011, 2: 446-450.
- [15] Y. Wang, Y. Di, M. Antonietti, et al. Excellent Visible-Light Photocatalysis of Fluorinated Polymeric Carbon Nitride Solids. *Chemistry of Materials*, 2010, 22: 5119-5121.
- [16] Y. Xu, and S.-P. Gao. Band gap of C<sub>3</sub>N<sub>4</sub> in the GW approximation. *International Journal of Hydrogen Energy*, 2012, 37: 11072-11080.
- [17] Y. Sun, Q. Wu, and G. Shi. Graphene based new energy materials. *Energy & Environmental Science*, 2011, 4: 1113-1132.
- [18] J. Xu, L. Luo, G. Xiao, et al. Layered C<sub>3</sub>N<sub>3</sub>S<sub>3</sub> polymer/graphene hybrids as metal-free catalysts for selective photocatalytic oxidation of benzylic alcohols under visible light. *ACS Catalysis*, 2014, 4: 3302-3306.
- [19] Z. Zhang, J. Long, L. Yang, et al. Organic semiconductor for artificial photosynthesis: water splitting into hydrogen by a bioinspired C<sub>3</sub>N<sub>3</sub>S<sub>3</sub> polymer under visible light irradiation. *Chemical Sciences*, 2011, 2: 1826-1830.
- [20] H.-Y. Xu, W.-C. Liu, J. Shi, et al. Photocatalytic discoloration of Methyl Orange by anatase/schorn composite: optimization using response surface method. *Environmental Science and Pollution Research*, 2014, 21: 1582-1591.
- [21] M. Fathinia, A. R. Khataee, M. Zarei, et al. Comparative photocatalytic degradation of two dyes on immobilized TiO<sub>2</sub> nanoparticles: Effect of dye molecular structure and response surface approach. *Journal of Molecular Catalysis A: Chemistry*, 2010, 333: 73-84.